

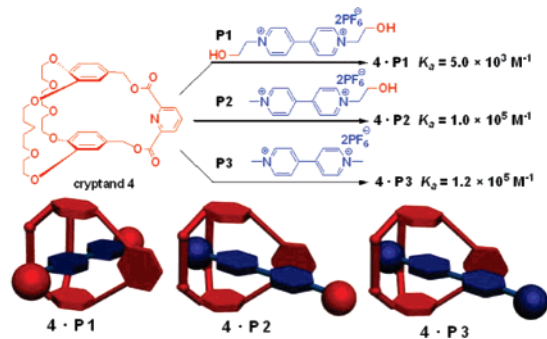
Paraquat Substituent Effect on Complexation with a Dibenzo-24-crown-8-Based Cryptand

Jinqiang Zhang,[†] Feihe Huang,^{*,†} Ning Li,[†] Hong Wang,[‡] Harry W. Gibson,^{*,‡} Peter Gantzel,[§] and Arnold L. Rheingold[§]

Department of Chemistry, Zhejiang University, Hangzhou 310027, People's Republic of China, Department of Chemistry, Virginia Polytechnic Institute and State University, Blacksburg, Virginia 24061-0212, and Department of Chemistry and Biochemistry, University of California, San Diego, La Jolla, California 92093-0358

fhuang@zju.edu.cn; hwgibson@vt.edu

Received August 2, 2007



Dibenzo-24-crown-8-based cryptand **4** forms 1:1 inclusion complexes with three paraquat derivatives, **P1**, **P2**, and **P3**, as demonstrated by proton NMR spectroscopy and X-ray analysis. However, it was found that methyl-substituted paraquat derivatives, **P2** and **P3**, can bind cryptand **4** more strongly than non-methyl-substituted paraquat derivative **P1**. The association constants (K_a) were determined in acetone by using a UV–vis titration method to be $5.0 \times 10^3 \text{ M}^{-1}$ for **4**·**P1**, $1.0 \times 10^5 \text{ M}^{-1}$ for **4**·**P2**, and $1.2 \times 10^5 \text{ M}^{-1}$ for **4**·**P3**, respectively. In the solid state, **4**·**P2** and **4**·**P3** have similar T-type inclusion complexation conformations, which are very different from the pseudorotaxane-type complexation conformation of **4**·**P1**. Theoretical calculations were done to explain these experimental results.

In supramolecular chemistry, the control of the direction of incorporation of a guest into a host (or threading of a host onto a guest) and the relative positional changes that take place within the complexes is very important for the construction of molecular machines and preparation of information storage materials.¹ Fujita et al. observed that the guest rotation can be significantly restricted by the distortion of a cyclodextrin

cavity.^{1a} Schalley et al. found that small structural changes such as the simple exchange of a CH group by an isoelectronic N atom can cause unexpectedly large effects on the deslipping reaction of rotaxanes.^{1d} Harada et al. revealed that the direction of threading cyclodextrins onto alkyl pyridinium derivatives can be kinetically controlled.^{1j}

Paraquat derivatives (*N,N'*-dialkyl-4,4'-bipyridinium salts) have been widely used as both hosts and guests in supramolecular chemistry.² The pursuit of high binding ability with paraquat derivatives and the facile synthesis of the precursors have led us to synthesize dibenzo-24-crown-8-based cryptands. Previously, we found that *cis*- and *trans*-dibenzo-24-crown-8-based cryptands form pseudorotaxane-type inclusion complexes with a bis(β -hydroxyethyl)-substituted paraquat salt **P1**.³

Here we report complexation studies between a *cis*-dibenzo-24-crown-8-based cryptand (**4**) and two methyl-substituted paraquat derivatives (**P2** and **P3**) and the comparison of these two complexes with the complex of cryptand **4** with **P1**. We found that methyl substitution can affect not only host–guest binding strength but also how the guest is incorporated into the host–guest inclusion complex in the solid state.

The *cis*-dibenzo-24-crown-8-based cryptand **4**³ and paraquat derivatives **P1**,⁴ **P2**,⁵ and **P3**⁶ with different *N*-substituents were

(1) (a) Chen, W. H.; Fukudome, M.; Yuan, D. Q.; Fujioka, T.; Mihashi, K.; Fujita, K. *Chem. Commun.* **2000**, 541–542. (b) Harada, A. *Acc. Chem. Res.* **2001**, *34*, 456–464. (c) Tseng, H.-R.; Vignon, S. A.; Stoddart, J. F. *Angew. Chem., Int. Ed.* **2003**, *42*, 1491–1495. (d) Felder, T.; Schalley, C. A. *Angew. Chem., Int. Ed.* **2003**, *42*, 2258–2260. (e) Onagi, H.; Blake, C. J.; Easton, C. J.; Lincoln, S. F. *Chem. Eur. J.* **2003**, *9*, 5978–5988. (f) Badjic, J. D.; Balzani, V.; Credi, A.; Silvi, S.; Stoddart, J. F. *Science* **2004**, *303*, 1845–1849. (g) Hernandez, J. V.; Kay, E. R.; Leigh, D. A. *Science* **2004**, *306*, 1532–1537. (h) Scarso, A.; Onagi, H.; Rebek, J., Jr. *J. Am. Chem. Soc.* **2004**, *126*, 12728–12729. (i) Scarso, A.; Trembleau, L.; Rebek, J., Jr. *J. Am. Chem. Soc.* **2004**, *126*, 13512–13518. (j) Oshikiri, T.; Takashima, Y.; Yamaguchi, H.; Harada, A. *Chem. Eur. J.* **2007**, *13*, 7091–7098.

(2) Huang, F.; Fronczek, F. R.; Gibson, H. W. *J. Am. Chem. Soc.* **2003**, *125*, 9272–9273. Huang, F.; Gibson, H. W.; Bryant, W. S.; Nagvekar, D. S.; Fronczek, F. R. *J. Am. Chem. Soc.* **2003**, *125*, 9367–9371. Huang, F.; Jones, J. W.; Slobodnick, C.; Gibson, H. W. *J. Am. Chem. Soc.* **2003**, *125*, 14458–14464. Huang, F.; Gibson, H. W. *J. Am. Chem. Soc.* **2004**, *126*, 14738–14739. Huang, F.; Nagvekar, D. S.; Slobodnick, C.; Gibson, H. W. *J. Am. Chem. Soc.* **2005**, *127*, 484–85. Huang, F.; Switek, K. A.; Zakharov, L. N.; Fronczek, F. R.; Slobodnick, C.; Lam, M.; Golen, J. A.; Bryant, W. S.; Mason, P. E.; Rheingold, A. L.; Ashraf-Khorassani, M.; Gibson, H. W. *J. Org. Chem.* **2005**, *70*, 3231–3241. Schmidt-Schäffer, S.; Grubert, L.; Grummt, U. W.; Buck, K.; Abraham, W. *Eur. J. Org. Chem.* **2006**, 378–398. Huang, F.; Gantzel, P.; Nagvekar, D. S.; Rheingold, A. L.; Gibson, H. W. *Tetrahedron Lett.* **2006**, *47*, 7841–7844. Zong, Q.-S.; Chen, C.-F. *Org. Lett.* **2006**, *8*, 211–214. Han, T.; Chen, C.-F. *Org. Lett.* **2006**, *8*, 1069–1072. Huang, F.; Nagvekar, D. S.; Zhou, X.; Gibson, H. W. *Macromolecules* **2007**, *40*, 3561–3567. Alcalde, E.; Pérez-García, L.; Ramos, S.; Stoddart, J. F.; White, A. J. P.; Williams, D. J. *Chem. Eur. J.* **2007**, *13*, 3964–3979. Reviews: Harada, A. *Acta Polym.* **1998**, *49*, 3–17. Raymo, F. M.; Stoddart, J. F. *Chem. Rev.* **1999**, *99*, 1643–1664. *Molecular Catenanes and Knots*; Sauvage, J.-P.; Dietrich-Buchecker, C., Eds.; Wiley: New York, 1999. Mahan, E.; Gibson, H. W. In *Cyclic Polymers*, 2nd ed.; Semlyen, A. J., Ed.; Kluwer Publishers: Dordrecht, The Netherlands, 2000; pp 415–560. Hubin, T. J.; Busch, D. H. *Coord. Chem. Rev.* **2000**, *200*–202, 5–52. Panova, I. G.; Topchieva, I. N. *Russ. Chem. Rev.* **2001**, *70*, 23–44. Huang, F.; Gibson, H. W. *Prog. Polym. Sci.* **2005**, *30*, 982–1018.

(3) Gibson, H. W.; Wang, H.; Slobodnick, C.; Merola, J.; Kassel, W. S.; Rheingold, A. L. *J. Org. Chem.* **2007**, *72*, 3381–3393.

(4) Shen, Y. X.; Engen, P. T.; Berg, M. A. G.; Merola, J. S.; Gibson, H. W. *Macromolecules* **1992**, *25*, 2786–2787.

(5) Tundo, P.; Kippenberger, D. J.; Politi, M. J.; Klahn, P.; Fendler, J. H. *J. Am. Chem. Soc.* **1982**, *104*, 5352–5358.

(6) Luong, J. C.; Nadjo, L.; Wrighton, M. S. *J. Am. Chem. Soc.* **1978**, *100*, 5790–5795.

* Address correspondence to these authors. F.H.: fax +86-571-8795-1895, phone +86-571-8795-3189. H.W.G.: fax +01-540-231-8517, phone +01-540-231-5902.

[†] Zhejiang University.

[‡] Virginia Polytechnic Institute and State University.

[§] University of California, San Diego.

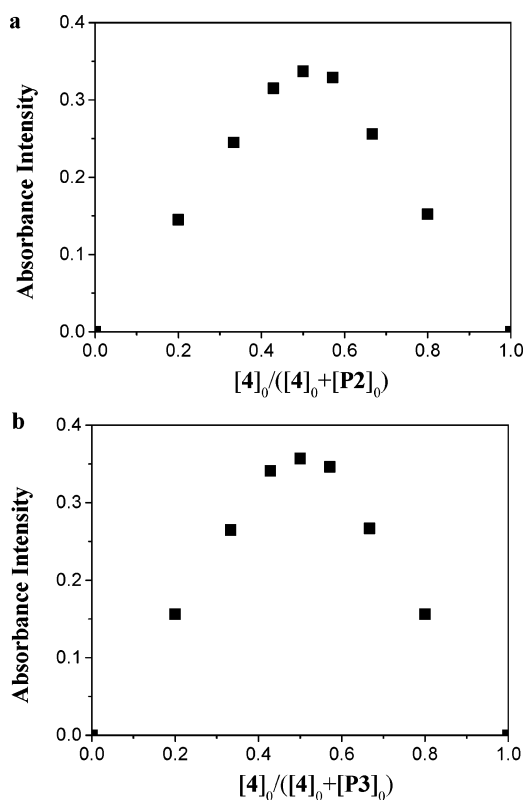
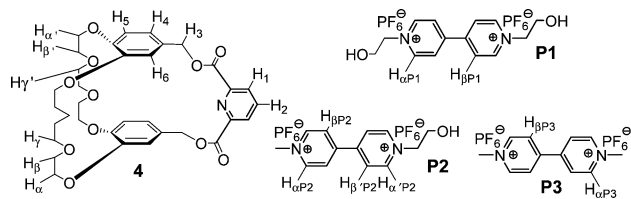


FIGURE 1. Job plots showing the 1:1 stoichiometries of the complexes between **4** and **P2** (a) and **4** and **P3** (b) in acetone by plotting the absorbance difference at $\lambda = 403$ nm (the host–guest charge-transfer band) against the mole fraction of **4**. $[4]_0$, $[P2]_0$, and $[P3]_0$ are initial concentrations of **4**, **P2**, and **P3**. $[4]_0 + [P2]_0 = [4]_0 + [P3]_0 = 1.00$ mM.

synthesized by literature procedures. Then the complexation between cryptand **4** and each of the three guests was studied. When equimolar (1.00 mM) acetone solutions of cryptand **4** and each of paraquat derivative salts **P1**, **P2**, and **P3** were made, a yellow color appeared due to charge transfer between electron-rich aromatic rings of the cryptand host and electron-poor pyridinium rings of the guest. And it was visually observed that the yellow color of the solution containing **P1** and cryptand **4** was not so deep as that of the other two solutions. This difference in the yellow color intensity gave us direct evidence that cryptand **4** binds **P1** not so strongly as it binds **P2** or **P3**.



Job plots⁷ based on UV–vis spectroscopy absorbance data of the charge-transfer band ($\lambda = 403$ nm) demonstrated that the complexes of cryptand **4** with **P2** and **P3** were of 1:1 stoichiometry in solution (Figure 1). As reported previously,³ the complex of cryptand **4** with **P1** also has a 1:1 stoichiometry in solution. The association constants were determined by probing the charge-transfer band of the complexes by UV–vis

(7) Job, P. *Ann. Chim.* **1928**, 9, 113–203.

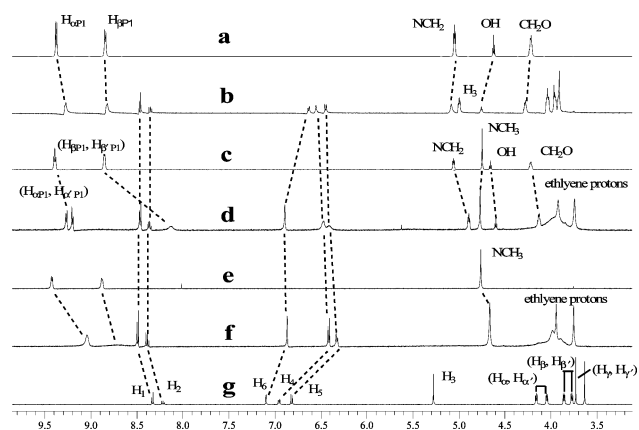


FIGURE 2. Partial proton NMR spectra (500 MHz, acetone- d_6 , 22 °C) of **P1** (a), 2.00 mM cryptand **4** and **P1** (b), **P2** (c), 2.00 mM cryptand **4** and **P2** (d), **P3** (e), 2.00 mM cryptand **4** and **P3** (f), and cryptand **4** (g).

spectroscopy and employing a titration method. Progressive addition of an acetone solution with high guest salt (**P1**, **P2**, or **P3**) concentration and low host (**4**) concentration to an acetone solution with the same concentration of host **4** results in an increase of the intensity of the charge-transfer band of the complex. Treatment of the collected absorbance data at $\lambda = 403$ nm with a nonlinear curve-fitting program afforded the corresponding association constants: $1.2 (\pm 0.4) \times 10^5 \text{ M}^{-1}$ for **4**·**P3**, $1.0 (\pm 0.3) \times 10^5 \text{ M}^{-1}$ for **4**·**P2**, and $5.0 (\pm 0.2) \times 10^3 \text{ M}^{-1}$ for **4**·**P1**.^{8,9} The large difference in association constants between complexes **4**·**P2** and **4**·**P3** and complex **4**·**P1** indicates that the methyl substitution has an important influence on the binding strength between *cis*-dibenzo-24-crown-8-based cryptand **4** and paraquat derivatives. This led us to further explore how the methyl substitution affects the host–guest complexation in solution by proton NMR spectroscopy, the host–guest organization in the solid state by single-crystal X-ray analysis, and why it has these effects by molecular modeling.

To investigate the complexation between cryptand **4** and the three paraquat derivatives, proton NMR spectra of equimolar (2.00 mM) deuterated acetone solutions of cryptand **4** with each of the three guests were examined. By comparison, it was found the spectra of solutions of **4** with **P2** and **P3** were different from that of the solution of **4** with **P1** (Figure 2). The peaks of some of the ethyleneoxy protons of cryptand **4** became broad after the complexation with methyl-substituted paraquat derivatives **P2** or **P3** (Figure 2, spectra d, f, and g), while clearly three peaks were observed for ethyleneoxy protons of cryptand **4** after complexation with **P1** (Figure 2, spectra b and g). Also β -pyridinium protons of **P2** and **P3** gave broad signals after complexation (Figure 2, spectra c, d, e, and f), while a relatively sharp peak was observed for β -pyridinium protons of **P1** after complexation (Figure 2, spectra a and b). On the basis of an

(8) Connors, K. A. *Binding Constants*; Wiley: New York, 1987. Corbin, P. S. Ph.D. Dissertation, University of Illinois at Urbana–Champaign, Urbana, IL, 1999. Ashton, P. R.; Ballardini, R.; Balzani, V.; Belohradsky, M.; Gandolfi, M. T.; Philp, D.; Prodi, L.; Raymo, F. M.; Reddington, M. V.; Spencer, N.; Stoddart, J. F.; Venturi, M.; Williams, D. J. *J. Am. Chem. Soc.* **1996**, 118, 4931–4951.

(9) The association constant for **4**·**P1** obtained here is lower than the reported value,³ $1.0 (\pm 0.1) \times 10^4 \text{ M}^{-1}$, which was determined based on ¹H NMR using the “Weber rule”: Weber, G. *Molecular Biophysics*; Pullman, B., Weissbluth, M., Eds.; Academic Press: New York, 1965; pp 369–397.

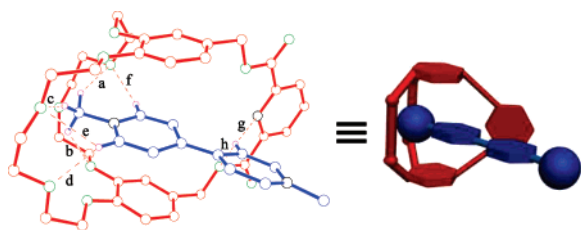


FIGURE 3. A ball-stick view of the X-ray structure of **4·P3**. **4** is red, **P3** is blue, hydrogens are magenta, oxygens are green, and nitrogens are black. PF_6^- counterions, solvent molecules, and hydrogens except the ones involved in hydrogen bonding between **4** and **P3** were omitted for clarity. Hydrogen bond¹² parameters: $\text{H}\cdots\text{O}$ (N) distance (Å), $\text{C}-\text{H}\cdots\text{O}$ (N) angle (deg), $\text{C}\cdots\text{O}$ (N) distance (Å)—**a**, 2.623, 149.6, 3.503; **b**, 2.507, 129.2, 3.217; **c**, 2.431, 157.1, 3.356; **d**, 2.262, 147.4, 3.105; **e**, 2.669, 135.1, 3.408; **f**, 2.388, 153.3, 3.266; **g**, 2.461, 141.5, 3.259; **h**, 2.652, 135.7, 3.397. The centroid–centroid distance (Å) and dihedral angle (deg) between the two catechol rings of cryptand **4**: 6.741, 16.64.

HMQC spectrum of a solution of **4** and **P2** (see the Supporting Information) and integration, the singlet at δ 4.76 ppm in Figure 2d can be assigned to the *N*-methyl protons of **P2**. Similarly the singlet at δ 4.66 ppm in Figure 2f can be assigned to the *N*-methyl protons of **P3**. The singlet for the benzylic protons H_3 of cryptand **4** disappeared after complexation with **P2** and **P3** (Figure 2, spectra d, f, and g).¹⁰ However, the singlet for the benzylic protons H_3 of cryptand **4** was observed at δ 4.99 ppm after complexation between **4** and **P1** (Figure 2, spectra b and g).¹¹

X-ray analyses were done on single crystals of complexes obtained by vapor diffusion of pentane into acetone solutions of cryptand **4** and each of the three paraquat derivative guests. In the solid state, **4·P2** and **4·P3** have similar T-type conformations, which are very different from the pseudorotaxane-type conformation of **4·P1**.³

In the crystal structure of 1:1 complex **4·P3** (Figure 3), the *N*-methyl group of paraquat guest **P3** is oriented into the dibenzo-24-crown-8 cavity and the complex has a T-type conformation. Complex **4·P3** is stabilized by eight hydrogen bonds. All three *N*-methyl hydrogen atoms of paraquat **P3** form effective hydrogen bonds with the ethyleneoxy oxygen atoms (**a**, **b**, and **c** in Figure 3) of cryptand **4**. Also two α -pyridinium hydrogen atoms form three hydrogen bonds with the ethyleneoxy oxygen atoms of the host (**d**, **e**, and **f** in Figure 3). One β -pyridinium hydrogen atom forms two hydrogen bonds with the pyridine nitrogen atom (**g** in Figure 3) and an ester oxygen atom on the host (**h** in Figure 3), respectively. Complex **4·P3** is stabilized also by face-to-face π -stacking and charge transfer interactions between the two electron-rich aromatic rings of the host and one of the two electron-poor pyridinium rings of the guest. The two catechol rings of host **4** are not parallel but rather have a dihedral angle of 16.64° and a centroid–centroid distance of 6.741 Å (Figure 3).

(10) It has been known for some time that some complexes of lariet ethers (Durst, H. D.; Echegoyen, L.; Gokel, G. W.; Kaifer, A. *Tetrahedron Lett.* **1982**, 23, 4449–4452. Echegoyen, L.; Parra, D.; Bartlotti, L. J.; Hanlon, C.; Gokel, G. W. *J. Coord. Chem.* **1988**, 18, 85–91) and cryptands (Schmidt, E.; Popov, A. I.; Kintzinger, J. P.; Tremillon, J.-M. *J. Am. Chem. Soc.* **1983**, 105, 7563–7566) display increased relaxation times, due to both “compression” and desolvation and the relaxation process being dominated by reorientational motion of the total complex. We hypothesize that this is the basis of the disappearance of the signal for the benzylic protons **4·P2** and **4·P3**.

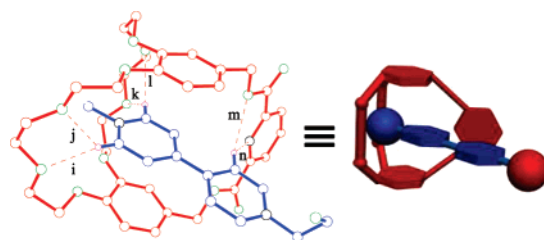


FIGURE 4. A ball-stick view of X-ray structure of **4·P2**. **4** is red, **P2** is blue, hydrogens are magenta, oxygens are green, and nitrogens are black. PF_6^- counterions, solvent molecules, and hydrogens except the ones involved in hydrogen bonding between **4** and **P2** were omitted for clarity. Hydrogen bond¹² parameters: $\text{H}\cdots\text{O}$ (N) distance (Å), $\text{C}-\text{H}\cdots\text{O}$ (N) angle (deg), $\text{C}\cdots\text{O}$ (N) distance (Å)—**i**, 2.350, 3.221, 152.0; **j**, 2.424, 133.6, 3.155; **k**, 2.557, 140.3, 3.344; **l**, 2.580, 149.7, 3.434; **m**, 2.556, 141.9, 3.354; **n**, 2.457, 142.2, 3.259. The centroid–centroid distance (Å) and dihedral angle (deg) between the two catechol rings of cryptand **4**: 6.740, 14.20.

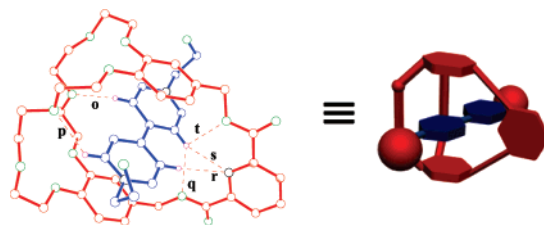


FIGURE 5. A ball-stick view of X-ray structure of **4·P1**.³ **4** is red, **P1** is blue, hydrogens are magenta, oxygens are green, and nitrogens are black. PF_6^- counterions, solvent molecules, and hydrogens except the ones involved in hydrogen bonding between **4** and **P1** were omitted for clarity. Hydrogen bond¹² parameters: $\text{H}\cdots\text{O}$ (N) distance (Å), $\text{C}-\text{H}\cdots\text{O}$ (N) angle (deg), $\text{C}\cdots\text{O}$ (N) distance (Å)—**o**, 2.317, 130.6, 3.023; **p**, 2.347, 133.9, 3.082; **q**, 2.535, 131.1, 3.239; **r**, 2.703, 175.9, 3.651; **s**, 2.402, 159.2, 3.307; **t**, 2.653, 101.1, 2.986. The centroid–centroid distance (Å) and dihedral angle (deg) between the two catechol rings of cryptand **4**: 6.890, 9.89.

The *N*-methyl group of paraquat guest **P2** is also oriented into the dibenzo-24-crown-8 cavity in the crystal structure (Figure 4) of the 1:1 complex **4·P2** in a T-type conformation similar to **4·P3** in the solid state. Complex **4·P2** is also stabilized by hydrogen bonding and face-to-face π -stacking and charge transfer interactions between the two electron-rich aromatic rings of host and one of the two electron-poor pyridinium rings of the guest. Also two α -pyridinium hydrogens are hydrogen bonded to ethyleneoxy oxygen atoms (**i**, **j**, **k**, and **l** in Figure 4) and one β -pyridinium hydrogen atom forms two hydrogen bonds with the pyridine nitrogen atom (**n** in Figure 4) and an ester oxygen atom on the host (**m** in Figure 4). However, none of the three methyl hydrogen atoms of **P3** are involved in hydrogen bonding between the host and guest (Figure 4). The two catechol rings are not parallel but rather have a dihedral angle of 14.20° and a centroid–centroid distance of 6.740 Å, which are very close to the above-mentioned corresponding values, 16.64° and 6.741 Å, for **4·P3**.

As reported previously, in the solid state, the 1:1 complex **4·P1** (Figure 5)³ has a pseudorotaxane-type conformation, which is significantly different from the above-mentioned T-type conformations of **4·P3** and **4·P2** in the solid state (Figures 3 and 4). Here non-methyl-substituted paraquat derivative guest

(11) The different behavior must be a consequence of the differing structures of the complexes; see the discussion of Figures 3–5.

